

Est.
1841

YORK
ST JOHN
UNIVERSITY

Sun, Chuanzhe, Zhong, Jicheng, Pan, Gang, Mortimer, Robert, Yu, Juhua, Wen, Shuailong, Zhang, Lei, Yin, Hongbin and Fan, Chengxin (2023) Controlling internal nitrogen and phosphorus loading using Ca-poor soil capping in shallow eutrophic lakes: Long-term effects and mechanisms. *Water Research*, 233. p. 119797.

Downloaded from: <https://ray.yorks.ac.uk/id/eprint/7545/>

The version presented here may differ from the published version or version of record. If you intend to cite from the work you are advised to consult the publisher's version:
<http://dx.doi.org/10.1016/j.watres.2023.119797>

Research at York St John (RaY) is an institutional repository. It supports the principles of open access by making the research outputs of the University available in digital form. Copyright of the items stored in RaY reside with the authors and/or other copyright owners. Users may access full text items free of charge, and may download a copy for private study or non-commercial research. For further reuse terms, see licence terms governing individual outputs. [Institutional Repositories Policy Statement](#)

RaY

Research at the University of York St John

For more information please contact RaY at
ray@yorks.ac.uk

1 Controlling internal nitrogen and phosphorus loading using
2 Ca-poor soil capping in shallow eutrophic lakes: Long-term
3 effects and mechanisms

4

5 Chuanzhe Sun^{a,e}, Jicheng Zhong^{a,*}, Gang Pan^{b,c}, Robert J.G. Mortimer^b, Juhua Yu^{a,d},
6 Shuailong Wen^{a,e}, Lei Zhang^a, Hongbin Yin^a, Chengxin Fan^a

7

8 ^a State Key Laboratory of Lake Science and Environment, Nanjing Institute of
9 Geography and Limnology, Chinese Academy of Sciences, Nanjing 210008, PR
10 China

11 ^b School of Humanities, York St John University, Lord Mayor's Walk, York, YO31
12 7EX, UK

13 ^c School of Chemical and Environmental Sciences, Guangdong Ocean University,
14 Zhanjiang 524088, China

15 ^d Institute of Soil and Fertilizer, Fujian Academy of Agricultural Sciences, Fuzhou,
16 350013, PR China

17 ^e University of Chinese Academy of Sciences, Beijing 100049, PR China

18

19

20 * Corresponding author:

21 Name: Jicheng Zhong

22 E-mail address: jczechong@niglas.ac.cn

23 Tel: +86-25-86882212; Fax: +86-25-57714759

24

25

26

27

28

29

30

31

32

33 **Abstract**

34 Clean soil is a potential capping material for controlling internal
35 nutrient loading and helping the recovery of macrophytes in eutrophic
36 lakes, but the long-term effects and underlying mechanisms of clean soil
37 capping under in-situ conditions remain poorly understood. In this study, a
38 three-year field capping enclosure experiment **combining** intact sediment
39 core incubation, in-situ porewater sampling, isotherm adsorption
40 experiments and analysis of sediment nitrogen (N) and phosphorus (P)
41 fractions was conducted to assess the long-term performance of clean soil
42 capping on internal loading in Lake Taihu. Our results indicate that clean
43 soil has excellent P adsorption and retention capacity as an ecologically
44 safe capping material and can effectively mitigate NH_4^+ -N and SRP
45 (**soluble reactive P**) fluxes at the sediment-water interface (**SWI**) and
46 porewater SRP concentration for one year after capping. The mean NH_4^+ -N
47 and SRP fluxes of capping sediment were $34.86 \text{ mg}\cdot\text{m}^{-2}\cdot\text{h}^{-1}$ and -1.58
48 $\text{mg}\cdot\text{m}^{-2}\cdot\text{h}^{-1}$, compared $82.99 \text{ mg}\cdot\text{m}^{-2}\cdot\text{h}^{-1}$ and $6.29 \text{ mg}\cdot\text{m}^{-2}\cdot\text{h}^{-1}$ for control
49 sediment. Clean soil controls internal NH_4^+ -N release through cation
50 (mainly Al^{3+}) exchange mechanisms, while for SRP, clean soil can not only
51 react with SRP due to its high Al and Fe content, but also stimulate the
52 migration of active Ca^{2+} to the capping layer, thus precipitating as
53 **Ca-bound P (Ca-P)**. Clean soil capping also contributed to the restoration
54 of macrophytes during the growing season. However, the effect of
55 controlling internal nutrient loading only lasted for one year under in-situ
56 conditions, after which the sediment properties returned to pre-capping
57 conditions. Our results highlight that clean Ca-poor soil is a promising
58 capping material and further research is needed to extend the longevity of
59 this geoengineering technology.

60 **Key words:**

61 Eutrophication; Internal nutrient loading; Capping; Ca-poor clean soil;
62 Sediment-water interface; Shallow lakes

63 **1. Introduction**

64 Eutrophication of lakes arising from excessive nitrogen (N) and
65 phosphorus (P) input leads to harmful algal blooms and retrogressive lake
66 evolution (Bullerjahn et al., 2016). The algae compete for light with
67 submerged vegetation, causing a shift from a macrophyte-dominated lake
68 to algae-dominated. This leads to degradation of the physical and chemical
69 environment beyond the point where self-recovery is possible, with the
70 lake becoming green, turbid and foul-smelling, and potentially threatening
71 drinking water sources (Guo, 2007; Scheffer and Nes, 2007).
72 Geo-engineering solutions typically focus on controlling the input of
73 external nutrients, however even once these are reduced or stopped there
74 can be persistent release of internal N and P loads that may continue to
75 cause eutrophication for years or even decades (Spears et al., 2014; Watson
76 et al., 2016).

77 Research has shown that both N and P can be limiting nutrients, and
78 hence controlling both is the most effective way to limit eutrophication
79 (Cotner, 2017; Paerl et al., 2016). In-situ capping of lake bed sediment is
80 considered a cost-effective technology for effectively isolating sediment
81 nutrients and preventing or severely reducing their release (Gu et al., 2017;
82 Lurling et al., 2016). Capping materials can include artificially
83 chemically-modified adsorbents such as lanthanum-modified bentonite
84 PhoslockTM (Copetti et al., 2016), iron-modified zeolite (Zhan et al., 2019),
85 and hydrous aluminum oxide (Li et al., 2017). However, depending on the
86 pH of the lake, these can lead to undesired chemical releases, including of
87 toxic trivalent aluminum ions (Al^{3+}) at $\text{pH} < 6$, or release of lanthanum
88 (Peterson et al., 1976; Figueiredo et al., 2022). Capping materials that
89 cause conditions to become more alkaline can lead to the conversion of
90 $\text{NH}_4^+\text{-N}$ into NH_3 , which is toxic to biota. Balancing the available active
91 ions in a chemically-modified capping layer with the available nutrients
92 that need locking up (e.g. SRP) is difficult but important because excess

93 capping material capacity will lead to potential toxicity from the Al/La and
94 NH₃ (Gibbs and Hickey, 2018). Iron-modified capping materials can be
95 effective but they tend to form sediment Fe-P which is easily dissolved and
96 released under seasonal hypoxia (Yang et al., 2020). The use of natural
97 clean soil as a capping material can avoid these potential toxic chemical
98 side effects, reducing both internal nutrient release and sediment
99 resuspension with excellent ecological safety (Pan et al., 2012a; Zhong et
100 al., 2022).

101 Evaluation of the efficiencies of capping materials for preventing
102 nutrient release are generally conducted under laboratory conditions,
103 and/or with short term small-scale field trials. Both approaches are limited
104 because natural lakes are subject to seasonal and episodic hydrodynamic
105 and temperature fluctuations, which in turn alter the sediment stability and
106 lake biogeochemistry significantly. Longer term field testing is essential to
107 thoroughly test the efficacy of capping approaches to control internal
108 loading.

109 Shallow lakes are characterized by frequent hydrodynamic
110 disturbances that lead to resuspension and deposition of bed sediments and
111 the deposition of nutrient-rich suspended particular matter (SPM) (Xu et
112 al., 2017). This presents a challenge for using capping layers to control
113 internal release of nutrients because these caps themselves can be
114 remobilized (Liu et al., 2019; Liu et al., 2016). Re-suspension events
115 create fresh sediment-water interfaces that can be highly reactive, leading
116 to a pulse of nutrients being released. At the same time, the material that is
117 removed becomes SPM, mainly comprised of inorganic metal-enriched
118 particles and organic matter, with large reactive surface area for binding
119 any dissolved N and P. These particles, and any nutrients they have
120 scavenged, then settle out of the water column to be re-deposited on top of
121 the newly formed sediment-water interface, ultimately burying it again
122 (Huser et al., 2016; Yu et al., 2017). Lakes that are subject to significant

123 input of external SPM will have the potential for this particulate material
124 to remove nutrients from the water column into the bed sediment, where
125 they may later become released once buried and conditions **change**.

126 The long-term effectiveness of **sediment capping under** in-situ lake
127 environments is poorly understood (Lin et al., 2019). Hence, in this study,
128 a three-year experimental monitoring approach was adopted, with in-situ
129 control enclosures (uncapped) compared against enclosures where the
130 sediment was capped with clean soil. Nutrient fluxes, porewater nutrient
131 profiles and nutrient fraction transformations were monitored to
132 understand nutrient dynamics and the impact of capping. The aim was to
133 understand the impact of long term in-situ capping with clean soil on
134 nutrient release and hence to provide a reference point for this approach to
135 the management of waterbody eutrophication.

136 **2. Materials and Methods**

137 **2.1 Site and material description**

138 The field enclosure experiment was conducted in Shiba Bay (Fig. 1) in
139 the northern part of Lake Taihu, China. Lake Taihu is situated on the
140 Yanqztze delta in a highly industrialized and economically developed area
141 of eastern China. The lake is relatively shallow (~1.5m), impacted by the
142 southeast monsoon, and prone to annual cyanobacterial blooms, severe
143 algal deposition, and water quality problems, which have led to the severe
144 accumulation of internal nutrient loading (Qin et al., 2007).

145 The clean soil material used for capping was collected on the shore of
146 Shiba Bay at Wuxi City, air dried and passed through a 40 mesh (380 μm)
147 screen before being applied. Table 1 shows its detailed composition,
148 notably, clean soil has a lower Ca content than the native lake sediments.

149 **2.2 Field enclosure experiment design and sampling**

150 **Fig.1** shows the location of the field enclosures and the sampling sites
151 within the enclosures. A **~70000 m² treatment and a ~50000 m² control**
152 **enclosure were** constructed with polyvinyl chloride (PVC), aiming to

153 prevent material exchange with the external water body. In the treatment
154 enclosure, several sub-enclosures were established, including clean sand,
155 Ca-poor soil, chitosan modified soil capping, etc. For Ca-poor soil capping
156 treatment, pre-processed clean soil for capping was sprayed into one
157 enclosure water body and left to sink to the surface of the sediment,
158 producing a capping layer of 5 cm to 10 cm thickness (Fig. S1). This
159 capping layer depth was based on our previous experimental work to
160 prevent resuspension (Pan et al., 2012a; Pan et al., 2019), which suggested
161 a minimum of 1cm, and the aim to allow macrophyte growth, which
162 requires 5-10cm for establishment and anchoring of roots. The control
163 enclosure without capping was located adjacent to the capping enclosure.

164 Capping was undertaken in January 2010. In-situ porewater samples
165 were collected 450d, 360d, 150d and 90d prior to capping and both
166 porewater samples and intact sediment cores were collected 60 d and 30 d
167 pre-capping, as well as 30d, 60d, 90d, 180d, 270d, 360d, 480d, 570d and
168 660d post-capping. The in-situ porewater equilibration sampling devices
169 (Peepers) were placed through the SWI by fixing to bamboo poles (Fig. S1)
170 and left to equilibrate for 15 d before being retrieved. Intact sediment cores
171 were sampled using a gravity core sampler (90 mm diameter, 60 cm length,
172 Rigo Co. Ltd., Japan). All porewater samples and sediment cores were
173 transported to the laboratory within 6 h for subsequent experiments.
174 Incubation experiments on intact sediment cores were used to measure
175 fluxes of $\text{NH}_4^+\text{-N}$ and SRP at the SWI under in-situ temperature and DO
176 conditions. Details of the sediment core incubations and in-situ peeper
177 experiments are given in the Supplementary material. Additionally,
178 triplicate sediment cores were also collected for the analysis of sediment
179 oxygen demand (SOD) using dissolved oxygen microprobe technology
180 (Presens, Regensburg, Germany). See our previous work for detailed
181 methods (Zhong et al., 2018).

182 **2.3 Sediment sampling and analysis**

183 After the sediment incubation experiments, the top 0-2 cm of the
184 sediment cores were sliced for surface sediment properties analysis. Fresh
185 sediment subsamples were used to analyze the total microbial activity of
186 sediments according to the method described by [Schnürer and Rosswall](#)
187 [\(1982\)](#). Then, three surface sediment samples were pooled and
188 homogenized to obtain a representative sample for further analysis. The
189 fresh surface sediment was lyophilized under a vacuum, and ground, then
190 passed through 0.150 mm sieves, and stored at 4 °C until subsequent
191 analysis.

192 The total nitrogen (TN) content of surface sediment was analyzed by
193 the alkaline potassium persulfate oxidation method ([Chinese EPA, 2002](#)).
194 Sediment dissolved inorganic nitrogen (DIN), including $\text{NH}_4^+\text{-N}$, $\text{NO}_3^-\text{-N}$
195 and $\text{NO}_2^-\text{-N}$ was extracted by 2 mol/L KCl and analyzed by UV
196 spectrophotometer ([Shannon et al., 2011](#)). Acid microwave digestion was
197 used to determine Al, Fe, Ca, Mn, Ni, Zn, Cu and Cr by ICP-AES ([Rukun,](#)
198 [1999](#)). Sediment organic matter content was measured as loss of ignition
199 (LOI) and determined by calcination at 550 °C for 6h. Sediment
200 phosphorus (P) fractions were extracted based on the method reported by
201 [Rydin \(2000\)](#) and were grouped as labile P ($\text{NH}_4\text{Cl-P}$), redox-sensitive P
202 (Fe-P), aluminum-bound P (Al-P), organic P (Org-P), other inorganic P
203 (Ca-P) and residual P (Res-P). Sediment total P was calculated as the sum
204 of above fractions. Further details of the extraction process are given in
205 [Fig. S2](#) in the supplementary materials.

206 **2.4 Phosphate adsorption isotherm experiments**

207 Phosphate adsorption isotherms were determined using the method
208 and calculation procedures in [Pan et al. \(2002; 2013\)](#) and [Yu et al. \(2017\)](#).
209 Briefly, 0.5g of the processed surface sediment was added to 40ml of the
210 solution, and mixed in 50ml polyethylene tube. The P concentration
211 gradient of the solutions was set to 0, 0.05, 0.2, 0.5, 1, 2, 5 and 10mg/L.
212 The mixture was incubated for 48h in a constant temperature shaker at 180

213 rpm and 25 °C. After the incubation, the supernatant was obtained by
214 centrifugation at 5000 rpm and filtered through a GF/C membrane for
215 analysis. Finally, the maximal adsorption capacity (Q_{\max} , mg/g) and zero
216 equilibrium P concentration (EPC_0 , mg/L) were calculated by the
217 non-linear form of the Langmuir equation to characterize the P adsorption
218 capacity of surface sediments.

219 **2.5 Statistical analysis**

220 One-way analysis of variance (ANOVA) with Tukey's post hoc test
221 was used to identify the significant differences in nutrient fluxes,
222 porewater nutrient concentrations, and sediment properties between control
223 and capping treatment. Pearson's correlation analysis was used to examine
224 the relationships between nutrient fluxes and environmental variables.
225 Significant difference was set at the $p < 0.05$ level. Statistical analysis was
226 performed using SPSS 25.0 (IBM, New York, USA).

227 **3. Results**

228 **3.1 Characteristics of clean soil and surface sediment**

229 The physicochemical characteristics of the clean soil and surface
230 sediment are shown in Table. 1 and Fig. 2. The results show that the clean
231 soil is characterized by lower organic matter (LOI), TP and TN and Ca
232 content with slightly higher Al and Fe content than the surface sediment
233 (Table. 1, Fig. 2). This plays a role in systematic differences measured
234 between the capping sediment and uncapped control sediment 30 days
235 post-capping, where the average values of the former are 95% LOI, 46%
236 TP, 52% TN, 31% (Ca), 110% (Al) and 130% (Fe) of those of the latter.
237 Furthermore, lower Mn, Ni, Zn, Cu and Zr contents were measured in the
238 clean soil, indicating its suitability as an ecologically safe capping material.
239 **When** the Ca-poor soil was introduced into the waterbody, the contents of
240 TP and Ca in the capping sediment **increased** rapidly within 60d after
241 capping, from 344 mg·kg⁻¹ and 2.02 mg·g⁻¹ to 644 mg·kg⁻¹ and 5.13 mg·g⁻¹,
242 respectively (Table. 1).

243 The sediment oxygen demand (SOD) of both capping and control
244 treatment showed significant seasonal variability within one year of
245 capping (Fig. S3). The highest SOD rates appeared in summer (180d) and
246 capping and control treatment only showed significant differences in
247 summer. The total microbial activity of the control sediment showed
248 significant seasonal variation (Fig. S4), and was highest in summer (180d),
249 while the capping sediments did not show significant seasonal variation.
250 Consequently, a significant difference between microbial activity in the
251 capping and control treatments was only found in summer.

252 **3.2 Fraction of N and P in capping and control sediments**

253 The variation of DIN of the surface sediment in control and capping
254 sediments is shown in Fig. 2. Sediment $\text{NH}_4^+\text{-N}$ content decreased
255 significantly after capping, reaching 57% of control sediment values 30d
256 post-capping, and then increased before further fluctuation. Sediment TN
257 also decreased post capping but then increased to levels similar to the
258 control. No significant difference was observed in $\text{NO}_3^-\text{-N}$ and $\text{NO}_2^-\text{-N}$
259 between control and capping sediment.

260 The variation of different P fractions in control and capping sediments
261 were displayed in Fig. 3 and Fig. S5. The dominant surface sediment P
262 fractions were Fe-P, Al-P and Ca-P prior to capping, averaging 27.20%,
263 24.55% and 22.49% respectively. The capped sediments then evolved such
264 that Al-P, Fe-P and Res-P became the dominant fractions (averaging
265 31.44%, 21.79% and 15.70% respectively). Furthermore, beyond 30d after
266 capping, the inert P (the sum of Al-P, Ca-P and Res-P) in the capping
267 sediment increased significantly compared with the control sediment,
268 averaging 62.60% of TP (Fig. S5). Sediment Ca-P content increased from
269 2.00 mg/kg at 30d post-capping to 104.29 mg/kg at 660d post-capping, a
270 50-fold increase respectively (Fig. 3).

271 Positive correlations ($p < 0.05$) were found between sediment Ca-P,
272 TP and Ca content, between Fe, Al and Res-P, and also between Al-P and

273 $\text{NH}_4^+\text{-N}$, and $\text{NH}_4^+\text{-N}$ and TN (Fig. S6). Significant negative correlations (p
274 < 0.05) were found between Res-P, Fe and Ca-P content and between Fe,
275 Al and $\text{NO}_3^-\text{-N}$ content, except for between Res-P and Fe, and Fe and Al
276 content in the sediment.

277 3.3 Phosphate adsorption capacity of capping and control sediments

278 A Langmuir model was used to fit the equilibrium adsorption data of
279 SRP on the surface sediment and clean capping soil (Pan et al., 2002),
280 results are shown in Fig. 4 and detailed parameters are listed in Table. S1.
281 EPC_0 of the capping sediments was significantly lower than that of the
282 control sediment. Furthermore, the Q_{\max} values for the control and capping
283 sediment were 0.2 mg/g to 0.31 mg/g and 0.24 mg/g to 0.35 mg/g,
284 respectively, and the clean soil was 0.36 mg/g. K_p values for retention
285 capacity of solid phase for SRP were 0.03 L/g to 0.54 L/g and 0.43 L/g to
286 4.27 L/g for the control and capping sediment respectively, and the clean
287 soil was 6.75 L/g. All the above parameters show that the capping sediment
288 was characterized by greater P adsorption and retention capacity than the
289 control sediment, except at the end of the 660-day experiment.

290 3.4 Nutrients porewater concentrations and fluxes across the SWI

291 The temporal variation of control and capping sediment porewater
292 nutrient concentrations with sediment depth are shown in Fig. 5. and Fig. 6.
293 For $\text{NH}_4^+\text{-N}$, the pre-capping sediments show a good degree of
294 homogeneity, with similar profiles of low overlying water concentrations
295 and then increasing concentrations with depth below the SWI reaching a
296 stable value at about -10cm, with steeper gradients during the warmer
297 sampling periods. Post-capping $\text{NH}_4^+\text{-N}$ profiles remain largely unchanged
298 in both control and capped systems, which show no significant differences.
299 For SRP, the pre-capping profiles show similar sharp increases in
300 concentration immediately below the SWI and generally peaked at about
301 -2cm to -5cm, with variations reflecting temperatures of sampling periods.
302 Post-capping profiles show clear differences between the control sites and

303 the capped sites. Capping caused burial of previous SRP peaks and then a
304 homogenization of profiles at lower levels of SRP which took a long period
305 (> 1 year) to re-establish diffusive gradients.

306 **Fig. 7.** shows $\text{NH}_4^+\text{-N}$ fluxes across the SWI in the control sediment
307 varied from $3.08 \pm 1.03 \text{ mg}\cdot\text{m}^{-2}\cdot\text{h}^{-1}$ to $300.68 \pm 53.95 \text{ mg}\cdot\text{m}^{-2}\cdot\text{h}^{-1}$, peaking
308 at 180d post-capping in summer. Capped sediments exhibited similar
309 temporal patterns, varying from $4.16 \pm 1.31 \text{ mg}\cdot\text{m}^{-2}\cdot\text{h}^{-1}$ to 107.57 ± 40
310 $\text{mg}\cdot\text{m}^{-2}\cdot\text{h}^{-1}$, with a peak at 180d, and second smaller peak (23.82 ± 12.11
311 $\text{mg}\cdot\text{m}^{-2}\cdot\text{h}^{-1}$) at 570d in summer. All measurements showed $\text{NH}_4^+\text{-N}$ efflux
312 from the sediment to the overlying water. Capping significantly ($p < 0.05$)
313 reduced $\text{NH}_4^+\text{-N}$ efflux for one year compared to control sediments, but
314 this effect disappeared thereafter.

315 SRP fluxes of control sediment (**Fig. 7**) show similar temporal trends
316 to $\text{NH}_4^+\text{-N}$ fluxes, varying from $0.24 \pm 0.04 \text{ mg}\cdot\text{m}^{-2}\cdot\text{h}^{-1}$ to 26.97 ± 1.91
317 $\text{mg}\cdot\text{m}^{-2}\cdot\text{h}^{-1}$, with a first peak at 180d post-capping and second smaller peak
318 ($9.93 \pm 4.10 \text{ mg}\cdot\text{m}^{-2}\cdot\text{h}^{-1}$) at 570d post-capping in summer. SRP fluxes in the
319 capped sediment switched from effluxes to influxes from 90d, reaching a
320 maximum influx of $-4.94 \pm 2.17 \text{ mg}\cdot\text{m}^{-2}\cdot\text{h}^{-1}$ at 180d post-capping, before
321 then switching back to effluxes, with a peak of $9.05 \pm 2.94 \text{ mg}\cdot\text{m}^{-2}\cdot\text{h}^{-1}$ at
322 570d. Fluxes were therefore significantly ($p < 0.05$) different to controls
323 for the first year, but this difference disappeared during the second year.
324 Notably, a significant ($p < 0.05$) positive correlation was obtained between
325 SRP flux and sediment Fe-P content (**Fig. S6**).

326 **4. Discussion**

327 **4.1 Clean soil capping controls $\text{NH}_4^+\text{-N}$ and SRP fluxes at the SWI**

328 In this study, **Fig. 7** shows that clean soil capping produces an average
329 of 31% reduction of internal $\text{NH}_4^+\text{-N}$ fluxes from the sediment for one year.
330 Simultaneously, capping caused SRP fluxes to switch from efflux to influx
331 for one year after capping, with the source-sink transition between
332 overlying water and sediment. Overall, clean soil capping effectively

333 controlled internal NH_4^+ -N and SRP release for up to one year, but not
334 thereafter.

335 The diffusion of N and P from sediment to overlying water mainly
336 depends on the concentration gradient at the SWI. Higher NH_4^+ -N fluxes
337 across the SWI consistent with higher porewater NH_4^+ -N concentrations
338 were measured in warm seasons (Fig. 7), where the elevated temperature
339 enhanced rates of microbial activity (Fig.S4), increasing the mineralization
340 of organic matter, depleting dissolved oxygen and enhancing anaerobic
341 conditions with sediment depth (Fig. S3) (Ding et al., 2018). A
342 combination of enhanced degradation of organic matter and reduced
343 nitrification caused increased accumulation of NH_4^+ -N, leading to steeper
344 pore-water gradients and enhanced efflux (Beutel, 2006; Zhong et al.,
345 2021). Reduced NH_4^+ -N effluxes in the capping sediment compared to the
346 control were likely due to the clean soil providing additional cation
347 exchange capacity that led to sorption of NH_4^+ -N when diffusing across the
348 capping layer. This ultimately reduced the NH_4^+ -N concentration of the
349 overlying water (Leyva-Ramos et al., 2008; Pan et al., 2012b; Zhan et al.,
350 2019).

351 In parallel, clean soil capping resulted in a reduction in porewater
352 SRP concentration and a switch from SRP effluxes to influxes. This result
353 is attributed to the immobilization of SRP by the clean soil. Prior to
354 capping, SRP was being liberated at depth due to anaerobic conditions,
355 most likely through a combination of release from degrading organic
356 matter and release from iron oxyhydroxides during microbial iron
357 reduction (Tammeorg et al., 2020). Addition of clean soil caused a
358 reduction in SRP generation at depth and led to the sediment becoming a
359 sink for P, thus the SRP concentration of the overlying water was
360 effectively reduced (Pan et al., 2012b, Pan et al., 2019). This is most likely
361 due to oxygenated soil containing abundant iron oxides and other reactive
362 surface sites causing simultaneous retardation of anerobic microbial

363 activity and sorption of SRP (Hinsinger, 2001; Moore et al., 1994). The
364 increased SRP influx during warmer sampling periods is likely due to
365 enhanced microbial degradation during those periods producing more SRP
366 available to be locked up by the sediment iron oxides (Figs 7, S3), and the
367 lack of accumulation of SRP in the pore-water suggests there are sufficient
368 iron oxides in the sediment to immediately adsorb any SRP produced. This
369 is further supported by the good SRP sorption and retention capacity of the
370 clean soil (Fig. 4; Table. S1). The above processes explain why SRP fluxes
371 were significantly positively correlated with sediment Fe-P content, with
372 smaller SRP influx at higher Fe-P content. Moreover, porewater SRP
373 concentrations of capping sediment within -10 cm reduced to range from
374 0.0005 mg·L⁻¹ to 0.40 mg·L⁻¹ compared to 0.04 mg·L⁻¹ to 1.84 mg·L⁻¹ in
375 control sediment, indicating the presence of a static layer directly below
376 the SWI after the clean soil capping, which has been confirmed to play a
377 key role in controlling internal P desorption and mobilization from the
378 sediment to overlying water across the SWI (Wang et al., 2017).

379 Temporally, the internal NH₄⁺-N and SRP fluxes recovered after one
380 year of capping. Our results suggest a continuous process of transformation
381 from clean soil to native sediment, leading to the return of
382 physicochemical properties towards those of the initial sediment (Table 1).
383 Recovered NH₄⁺-N fluxes may attributed to NH₄⁺-N being able to transfer
384 across the capping layer unhindered, as any cation capacity to absorb it
385 was used up. Meanwhile, a switch of SRP influxes to effluxes was detected,
386 corresponding with steeper SRP concentration gradient at the SWI (Fig. 6),
387 which supported the internal SRP release (Wen et al., 2020). This was
388 further supported by a weakening of the SRP sorption and retention
389 capacity effect of the clean soil (Fig. 4).

390 **4.2 Underlying mechanisms of clean soil capping to control porewater** 391 **NH₄⁺-N and SRP concentrations**

392 Our results show that clean soil can effectively control porewater SRP

393 concentration but not NH_4^+ -N concentrations (Fig. 5 and Fig. 6). Porewater
394 NH_4^+ -N concentration is significantly negatively correlated with the
395 sediment Al ion content (Fig. S6), thus we deduced that cation exchange
396 between the exchangeable cations in the clean soil (Al ion) and NH_4^+ -N in
397 porewater is an important mechanism for the adsorptive removal of
398 NH_4^+ -N from the porewater and controls its released from the clean soil
399 sediment caps (Alshameri et al., 2014; Lin et al., 2013; Lin et al., 2014).
400 This is supported by the fact that the clean soil has a higher Al and Fe
401 content than the sediment, and that this reduces with time (Table 1).
402 Finally, sediment NH_4^+ -N shares the same temporal variation with
403 sediment TN, and is also positively correlated with sediment Al-P content
404 (Fig. S6). This supports the hypothesis that NH_4^+ -N is adsorbed by the
405 clean soil. This process could release Al^{3+} , then promoting the reaction of
406 Al^{3+} and SRP in porewater to form Al-P (Fig. 8). Moreover, the aerobic
407 environment caused by clean soil capping could promote sediment
408 microbial activity, particularly nitrifying bacteria, thus NH_4^+ -N is
409 decreased in short term (Pan et al., 2019; Zhang et al., 2021). However, the
410 presence of a large amount of organic N in the sediment (Fig. 2) can
411 quickly replenish the porewater NH_4^+ -N concentration, which explains why
412 the clean soil capping has limited impact on porewater NH_4^+ -N
413 concentrations but can significantly reduce the NH_4^+ -N fluxes at the SWI.
414 Vertically, the NH_4^+ -N concentration in porewater increased with depth in
415 the sediment and reached a maximum stable value at -10 cm, which is
416 consistent with our previous study (Zhong et al., 2018). The highly
417 anaerobic conditions at depth are conducive to the accumulation of NH_4^+ -N
418 (Roberts et al., 2012), while nitrification is inhibited and denitrification
419 was promoted, thus promoting the desorption of NO_2^- -N, an intermediate
420 product of denitrification, from the sediment, explaining the negative
421 correlation of sediment NO_2^- -N and porewater NH_4^+ -N (Zhong et al., 2010a;
422 Zhong et al., 2010b). The possible explanation for the negative correlation

423 with sediment Res-P content was that capping leads to an increase in pH
424 which promotes the desorption and release of Res-P (Zhou et al., 2019).

425 Fig. 6 shows that clean soil capping is effective at controlling
426 porewater SRP. This can be attributed to the higher Fe content of the clean
427 soil (Table. 1). Previous studies have confirmed that the ligand exchange
428 of Fe oxide/hydroxide with SRP to form an inner-sphere P-O-Fe link plays
429 an important role in SRP uptake (Ajmal et al., 2018; Cao et al., 2016).
430 Furthermore, since SRP and $\text{NH}_4^+\text{-N}$ coexist in the porewater, it is possible
431 that the Al^{3+} can be desorbed from the clean soil via cation exchange
432 between Al^{3+} on the clean soil and porewater $\text{NH}_4^+\text{-N}$, allowing it to then
433 react with SRP to form Al-P (Fig. 8). Therefore, clean soil capping has a
434 better SRP adsorption capacity to control internal P release due in part to a
435 combination of the high Fe and Al present. This can be further supported
436 by the significant positive correlation between the sediment Fe and Al
437 content and sediment Res-P (Fig. S6), indicating that the presence of Fe
438 and Al can promote the formation of inert P which is consistent with the
439 result that lower SRP concentration was observed in the porewater (Zhan et
440 al., 2019). Notably, sediment Ca content increased from 1.99 mg/g to 5.32
441 mg/g over the whole experiment (Table. 1), and the migration of Ca could
442 accelerate the chemical precipitation of porewater SRP with Ca^{2+} to form
443 Ca-P, thereby transforming the porewater SRP to sediment inert P (Lin et
444 al., 2011). Therefore, we conclude that the control mechanism of porewater
445 SRP by clean soil capping was likely a combination of SRP adsorption due
446 to the higher Fe and Al content, and the co-precipitation of Ca^{2+} with
447 porewater SRP (Fig. 8). Clean soil capping can effectively reduce SRP
448 concentrations in porewater within one year, which was also confirmed by
449 our previous short-term work (Pan et al., 2019). However, the porewater
450 SRP concentrations recovered gradually after one-year post-capping due to
451 a combination of increased sediment P loading and the weakened P
452 adsorption and retention capacity (Fig. 4) (Wen et al., 2020).

453 **4.3 Variation of P fractions in surface sediments after capping**

454 Sediment P release potential is determined by various P fractions in
455 sediment and their relative abundance (Liu et al., 2022; Rydin, 2000). The
456 upper 2cm of the control and capping sediment contained different P
457 fractions (Fig. 3).

458 Sediment total P (TP) is the sum of different P fractions. Fig. 3 shows
459 that the TP of capping sediment increased significantly and approached
460 that in the control sediment within the first year after capping, while the
461 TP content of control sediment maintained high values throughout. This is
462 associated with the isotherm parameters determined by the Langmuir
463 equation, the Q_{\max} and K_p decrease from $0.36 \text{ mg}\cdot\text{g}^{-1}$ to $0.32 \text{ mg}\cdot\text{g}^{-1}$ and
464 $6.75 \text{ L}\cdot\text{g}^{-1}$ to $0.43 \text{ L}\cdot\text{g}^{-1}$ within one-year (Table. S1), suggesting the
465 reduced P adsorption and retention capacity of capping sediment, mainly
466 due to the reducing difference in the TP content compared to the control
467 sediment (Lai and Lam, 2009; Wen et al., 2020). The variations of different
468 P fractions in the capping sediment were significant. Previous studies have
469 confirmed that mobile P (the sum of $\text{NH}_4\text{Cl-P}$, Fe-P and Org-P) is
470 considered algal-available and hence a potential internal P loading while
471 inert P (the sum of Al-P , Ca-P and Res-P) is considered a pool of
472 permanent burial P which is hard to release (Rydin, 2000). Our results
473 showed that clean soil capping can significantly reduce the mobile P
474 content in the surface sediments (Fig. 3 and Fig. S5). $\text{NH}_4\text{Cl-P}$ corresponds
475 to immediately algal-available P, which is adsorbed to the surface of
476 sediment particles (Sun et al., 2009). An apparent reduction of $\text{NH}_4\text{Cl-P}$ in
477 capping sediment was observed, reducing from $3.97 \text{ mg}\cdot\text{kg}^{-1}$ to 1.43
478 $\text{mg}\cdot\text{kg}^{-1}$ compared to the control (Fig. 3), suggesting that clean soil capping
479 can effectively control labile P. This apparent decrease is attributed to the
480 introduction of clean soil characterized by excellent P adsorption capacity
481 that removes labile P by physical adsorption to soil particulates (Zhou et
482 al., 2019). This phenomenon is further supported by reduced porewater

483 SRP concentration within the clean soil capping layer.

484 Fe-P is redox-sensitive P, which easily released under anaerobic
485 conditions and transformed to potential algal-available P (Chen et al.,
486 2015). Fig. 3 and Fig. S5 show a decrease of mobile P in the capping
487 sediment mainly originated from Fe-P, accounting for 128.7% of decreased
488 mobile P and 92% of TP. The clean soil characterized by a high Fe that
489 promotes the reaction of Fe^{3+} with SRP to form Fe-P under aerobic
490 conditions during the cold season. And the lack of Ca-P together then
491 results in the increased ratio of mobile P to TP in the early period after
492 capping. Microbial activity and SOD were promoted by increased
493 temperatures (Figs. S3, S4), leading to anaerobic conditions within the
494 sediment during warm seasons, with Fe-P readily released due to the
495 reduction of Fe^{3+} to Fe^{2+} (Wang et al., 2016). Org-P increased slightly
496 early in the experiment but decreased during the warm season accompanied
497 by dissolution of Fe-P in the uncapped sediment, however, the opposite
498 variation was observed in capping sediment. This indicates different P
499 release mechanisms between control and capping sediment, the control
500 sediment being mainly controlled by coupled release of Fe-P and Org-P
501 while the capping sediment is dominated by the traditional Fe-P release
502 process, demonstrating the shift of internal P release processes after
503 capping (Liu et al., 2022; Sun et al., 2022). Notably, there is a negative
504 correlation between sediment Fe and Ca-P content, which gives the likely
505 explanation of competitive adsorption on P by stronger reactive Ca^{2+} and
506 Fe^{3+} , promoting the shift of Fe-P to Ca-P, a similar phenomenon to that
507 reported by Zhou et al. (2019).

508 Our results show that inert P increased sharply within one year of
509 capping (Fig. 3), which is mainly attributed to the increase of Ca-P and
510 Al-P. This result indicated that capping is beneficial for the formation of
511 inert P fractions in the sediment (Li et al., 2019; Yin et al., 2021), which is
512 further supported by the lower porewater SRP concentration observed in

513 the capping sediment (Fig. 6). Al-P is often analyzed together with Fe-P,
514 and while Al-P is actually more difficult to re-release than Fe-P, our result
515 found that sediment Al-P was positively correlated with sediment $\text{NH}_4^+\text{-N}$,
516 implying that the released Al^{3+} is from cation exchange between sediment
517 Al^{3+} and $\text{NH}_4^+\text{-N}$ in porewater, thus promoting the formation of Al-P
518 (Rönicke et al., 2021; Rydin, 2000). Furthermore, the Al-P content reduced
519 while the Ca-P content increased after 60d post-capping, which may be
520 attributed to the actively competitive adsorption of P by Ca^{2+} over Al^{3+}
521 (Yin et al., 2021). Ca-P is regarded as permanently buried P, and a
522 significant positive correlation was found between sediment Ca-P and Ca
523 content, consistent with our result that Ca-P accounts for 64.07% of the
524 increased TP during the experiment. In this study, Ca-poor soil exhibited a
525 similar excellent internal P control ability to Ca-modified material (Zhou
526 et al., 2019). The underlying mechanism is likely the formation of a Ca^{2+}
527 concentration gradient between the Ca-poor capping layer and native
528 surface sediment, which promotes the migration of active Ca^{2+} to the
529 capping layer and, thus, reacts with SRP to form a precipitate of Ca-P
530 compounds (Fig. 8). The above-mentioned shift in the release mechanism
531 of coupled Fe-P and Org-P to Fe-P suggests the transformation of
532 algae-dominated status to macrophyte-dominated status (Liu et al., 2022),
533 thus the precipitation of Ca and SRP by calcite crusts on the surface of
534 submerged macrophytes might play an important role in increased sediment
535 Ca-P (Blindow, 1992; Sand-Jensen et al., 2021). Furthermore, the reduced
536 sediment Res-P suggests the enhanced alkaline environment, which would
537 allow Ca^{2+} to become the primary SRP-binding reactant over Fe and Al,
538 and also explains the negative correlation of sediment Ca-P and Res-P
539 content (Wu et al., 2022).

540 **4.4 Implication for the development of Ca-poor capping material and** 541 **practical capping geoengineering**

542 In this study, the large-scale field experiment is close to a practical

543 geoengineering project, and hence understanding the long-term
544 performance is important for decision-making in eutrophication
545 management. The experimental results indicate that clean soil capping
546 could effectively mitigate internal N and P release from sediment
547 simultaneously for one year (Fig.7). Furthermore, clean soil is a natural
548 ecologically-safe material that helps to change the algae-dominated status
549 of a lake to macrophyte-dominated status (Pan et al., 2012a). In this study,
550 the recovery of submerged macrophytes was observed during the growing
551 season. Our results indicate that Ca-poor soil can be used in
552 geoengineering to control internal nutrient loading and provide a better
553 habitat for macrophytes. The dominant macrophytes observed were
554 naturally occurring *P. malaianus* and *P. crispus*, and their recovery was
555 accompanied by reduced Chl- α concentrations (Fig. S7) (Pan et al., 2012b).
556 Previous studies on capping materials have focused on calcium-rich
557 material, such as heat-modified Ca-rich attapulgite (Gan et al., 2009),
558 natural/modified zeolite (Zhan et al., 2019), illite (Gu et al., 2019) and
559 confirmed these have better capacity to control sediment internal P loading
560 and promote the transformation of mobile P to inert P (Hinsinger, 2001).
561 Therefore, use of clean soil characterized by lower Ca content was contrary
562 to the widely accepted view. Interestingly, we found that when Ca-poor
563 soil is introduced into the water body, the Ca-rich water body will
564 automatically supplement the Ca content to the capping layer, thus
565 achieving a similar effect to that of Ca-rich materials. This finding leads us
566 to consider the development of Ca-poor and environment-friendly
567 materials for geoengineering.

568 The time-limited effectiveness of geoengineering in controlling
569 internal nutrient loading continues to plague the successful application of
570 projects. We found that N and P fluxes accompanied with surface sediment
571 physicochemical properties recovered one-year post-capping (Fig. 7; Table
572 1). When the clean soil was introduced into the water body, the clean soil

573 gradually transformed to native sediment under the in-situ lake conditions.
574 For example, the Ca-rich water body will continually supply Ca to the
575 Ca-poor soil, thus causing changes in the P forms and Ca-P shifting
576 process (Fig. 3). In addition, considering the background of persistent
577 external inputs, the external input SPM has high nutrient and organic
578 matter content could continuously deposit upon the capping layer,
579 promoting the return of the physicochemical properties of new born SWI to
580 the pre-capping status (Wen et al., 2020). Furthermore, surface sediment is
581 prone to resuspension under hydrodynamic disturbance, which promotes
582 the potential for deposition of contaminated sediment from uncapped areas
583 to those with capping. Moreover, bioturbation will not only reorganize the
584 sediment vertically to allow the capping material to react with deep
585 sediment (Xu et al., 2017; Yin et al., 2021), but also can accelerate the
586 mixing of the deposited SPM and capping material, promoting the
587 sedimentation process of the capping material. Overall, we found that the
588 change in the color of surface sediment (clean soil) was slow as it
589 transformed from Ca-poor soil to native sediment after capping (Fig. S8).
590 However, the change in the contents of Ca and Ca-P in the surface
591 sediments (clean soil) was rapid (Table 1; Fig. 3). This result suggested
592 that the active migration of substances (such as Ca and P) in the water body
593 rather than sediment disturbance processes and external SPM input
594 dominated the recovery of sediment properties and internal loading.

595 Clean soil as a natural material can effectively control internal
596 loading of nutrients for only one year and promote macrophyte restoration
597 for a longer period. The results of our long-term enclosure experiment
598 cause us to worry about the long-term effects of other functional
599 geoengineering materials. Future research should focus on the long-term
600 effects of functional materials under field condition and how to use
601 management measures to extend the long-term effects of geoengineering
602 technology.

603 **5. Conclusion**

604 A three-year field enclosure experiment was carried out to investigate
605 the long-term performance and underlying mechanism of clean soil capping
606 on internal nutrient loading mitigation. Clean soil capping can not only
607 reduce internal N and P fluxes and porewater SRP concentration for one
608 year but also promote the restoration of macrophytes in a eutrophic lake.
609 Clean soil characterized with high Al and Fe content can prevent internal
610 NH_4^+ -N release through cation exchange, and also has excellent P
611 adsorption and retention capacity. Furthermore, Ca-poor clean soil has
612 performed better in the control of internal P release via not only high
613 cation capacity to react with SRP in the short-term, but also via stimulating
614 the migration of active Ca^{2+} to precipitate with SRP, thus promoting the
615 burial of internal P in long-term. However, under the in-situ conditions of
616 Lake Taihu, the properties of capping sediment will gradually recover to
617 the state of the native sediment, ultimately resulting in weakened
618 effectiveness after one-year post-capping. Our field enclosure experiment
619 demonstrated that the clean Ca-poor soil is a promising capping material to
620 control the internal nutrient loading and help the recovery of macrophytes,
621 and future research efforts should be exerted to extend the longevity of this
622 geoengineering technology.

623 **Acknowledgements**

624 The study was supported by Chinese National Basic Research Program
625 (2008CB418105), Chinese National Key Research and Development Program
626 (2022YFC3202703, 2022YFC3202705), and the National Natural Science Foundation
627 of China (Grant No. 41771516). We thank Guofeng Liu, Qiushi Shen, Jingge Shang,
628 and Mengyao Tang for their help in field sampling and experimental analysis. We also
629 thank the editor and anonymous reviewers for their constructive comments and
630 suggestions to help us improve the manuscript.

631

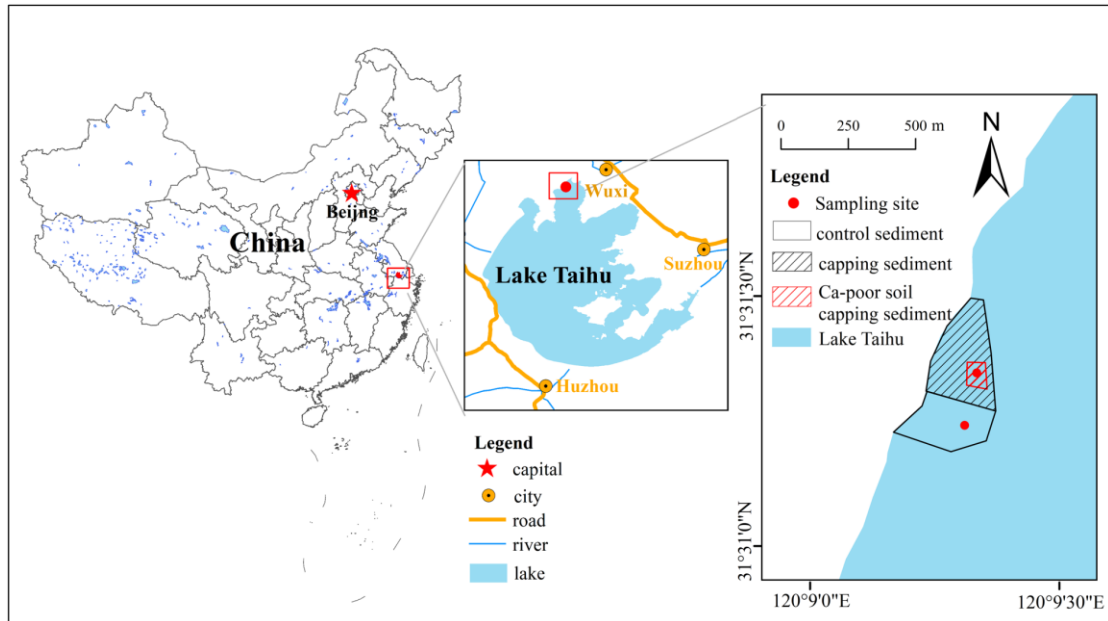
632

633
 634
 635
 636
 637
 638
 639
 640
 641
 642
 643
 644
 645
 646
 647
 648
 649
 650
 651
 652

653 **Table 1.** The physical and chemical properties of clean soil, control and capping
 654 sediment treatment during three-year experiment.

Sample	Time	LOI (%)	TP (mg/kg)	Al (mg/g)	Fe (mg/g)	Ca (mg/g)	Mn (mg/kg)	Ni (mg/kg)	Zn (mg/kg)	Cu (mg/kg)	Cr (mg/kg)
Clean soil		3.5	319	61.1	35.6	1.99	557	31	71	13	58
Control	60d pre-capping	3.7	779	55.1	27.3	6.98	902	75	259	98	111
Control	30d pre-capping	3.7	753	54.6	26.6	6.76	875	75	252	96	106
Control	30d post-capping	3.8	748	54.8	27.2	6.56	915	75	255	97	106
Control	60d post-capping	3.9	786	58.5	29.3	6.83	1006	79	264	97	119
Control	90d post-capping	4.2	781	60.1	30.1	7.17	974	79	268	103	122
Control	270d post-capping	4.2	703	53.6	26.7	6.40	835	54	195	83	115
Control	660d post-capping	4.2	647	53.9	26.7	6.78	815	64	220	84	99
Capping	60d pre-capping	4.6	816	59.3	29.1	6.38	938	78	260	101	118
Capping	30d pre-capping	4.6	855	59.8	29.7	6.55	959	78	266	101	122
Capping	30d post-capping	3.6	344	60.3	35.3	2.02	883	33	74	18	60
Capping	60d post-capping	4.0	644	58.7	31.5	5.13	873	60	200	70	99
Capping	90d post-capping	4.3	623	57.6	29.9	4.80	771	61	195	69	94
Capping	270d post-capping	4.5	609	52.5	25.0	5.21	737	61	197	70	90
Capping	660d post-capping	4.7	638	53.4	25.8	5.32	666	57	198	75	91

655
 656

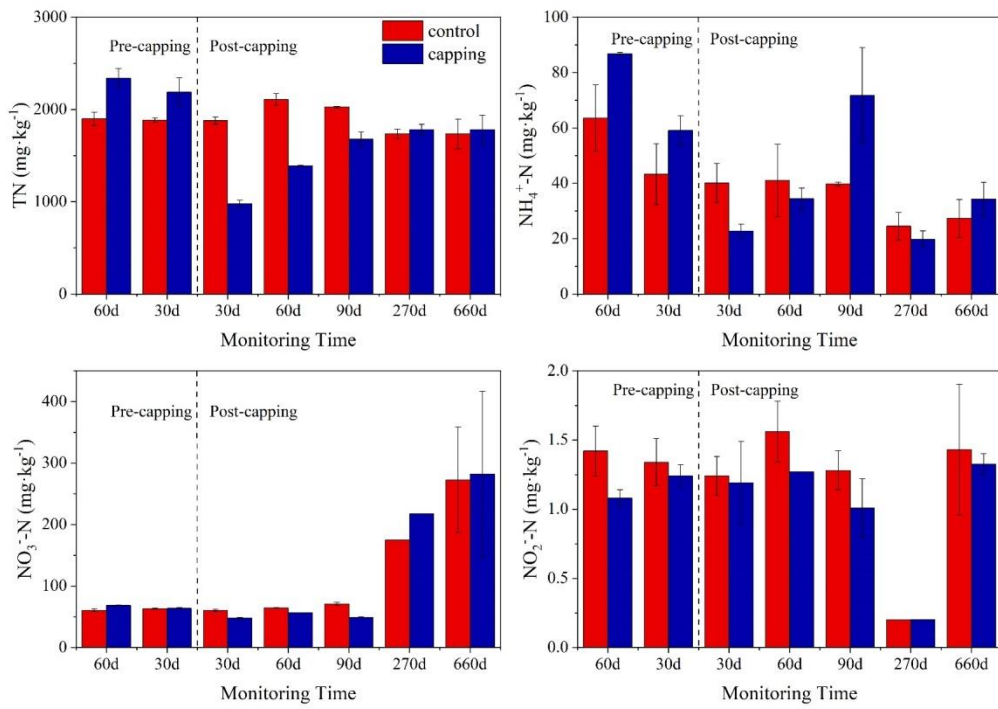


657

658

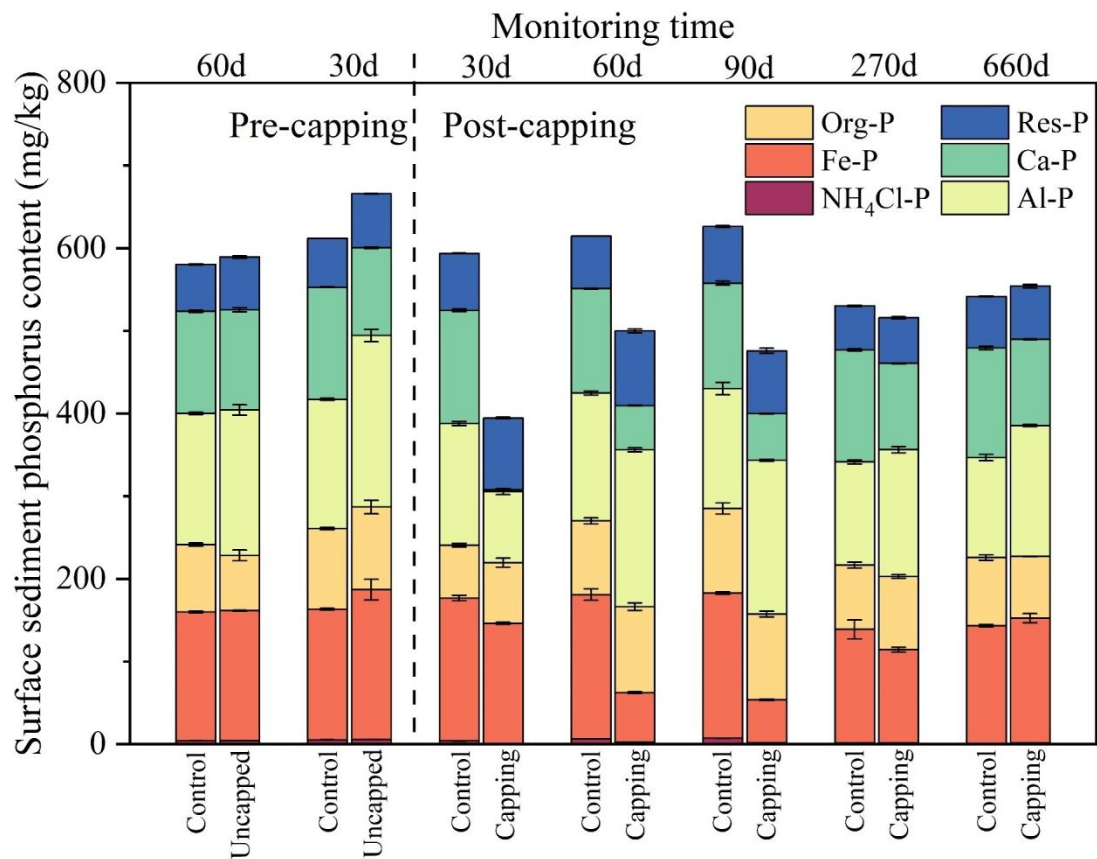
Fig. 1. Location of the field enclosure and the sampling sites in Lake Taihu.

659



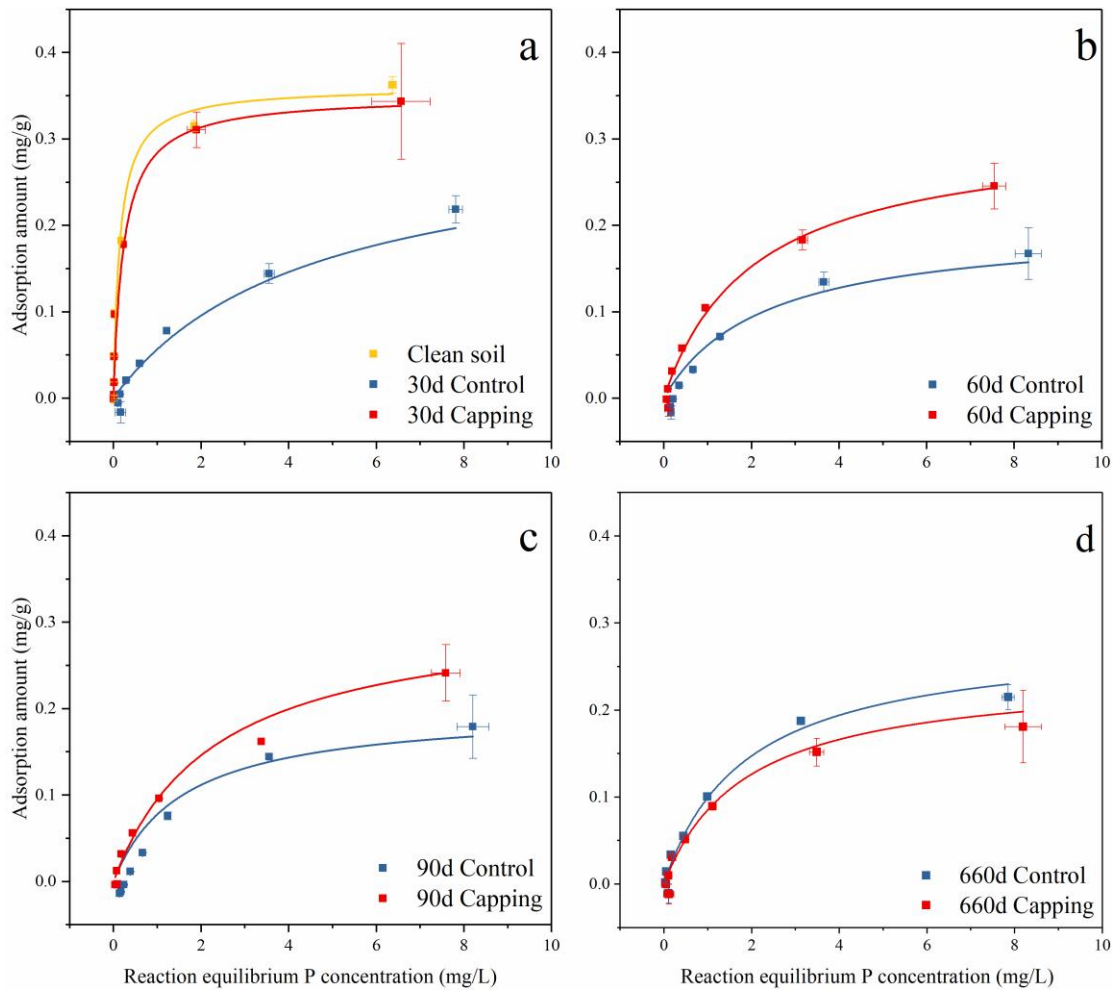
660
 661
 662
 663
 664

Fig. 2. TN and DIN in control and capping sediment treatment at seven sampling times.



665
666
667
668

Fig. 3. TP and P fractions in control and capping sediment at seven sampling times.



670

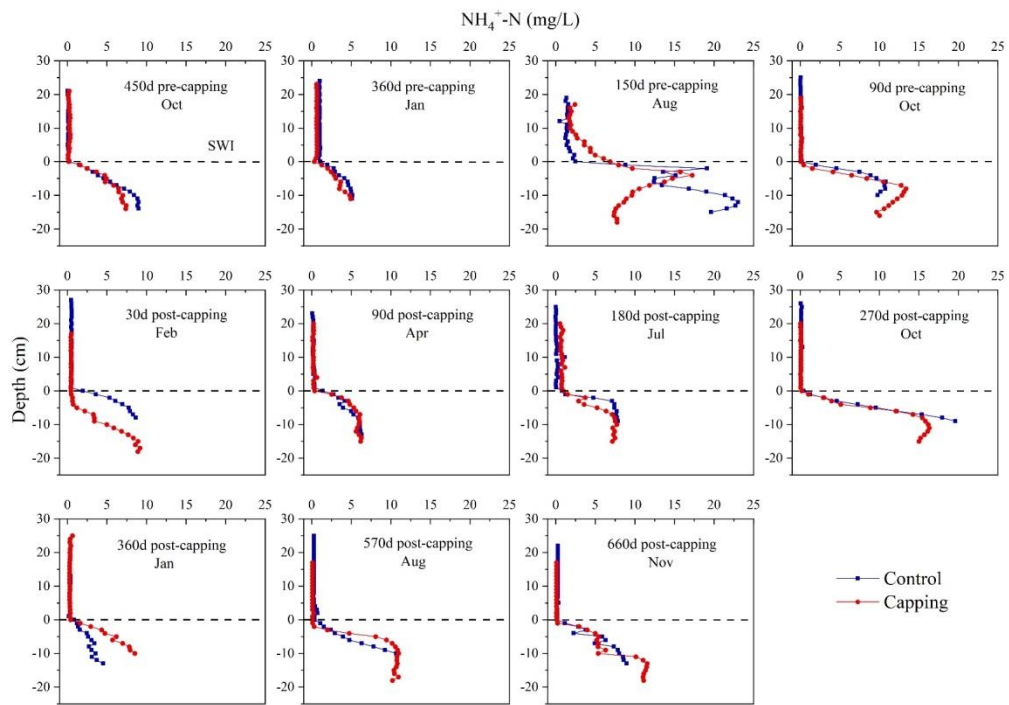
671

Fig. 4. Phosphorus adsorption isotherm regression for clean soil, control and capping sediment treatment using the non-linear form of the Langmuir equation.

672

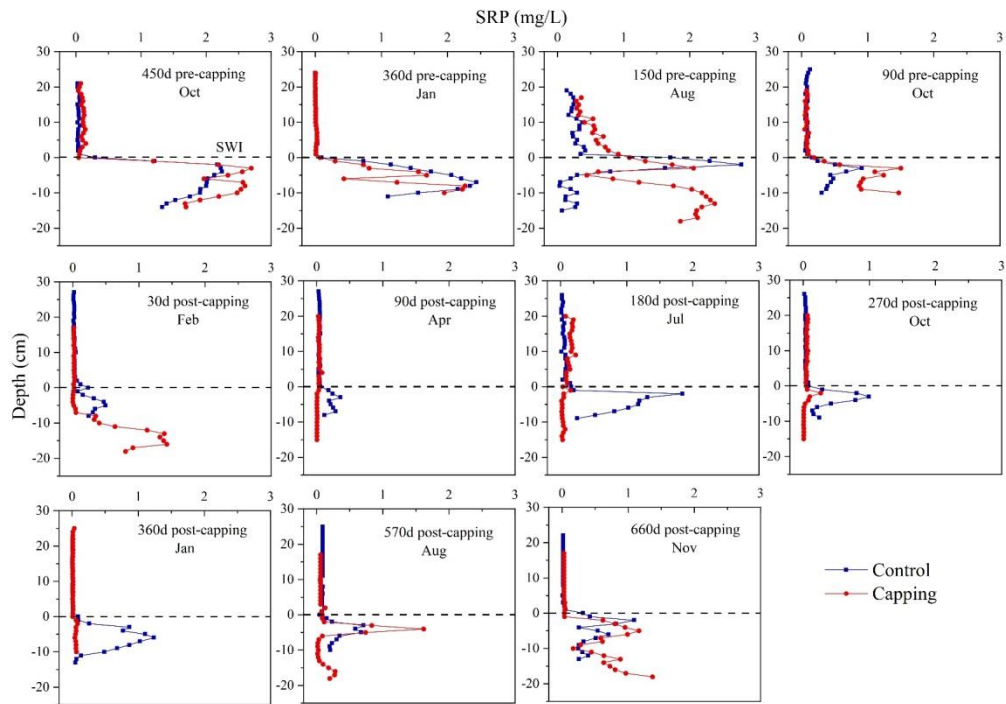
673

674



675
 676
 677

Fig. 5. $\text{NH}_4^+\text{-N}$ concentration in porewater profiles for control and capping sediment at eleven sampling times.



679

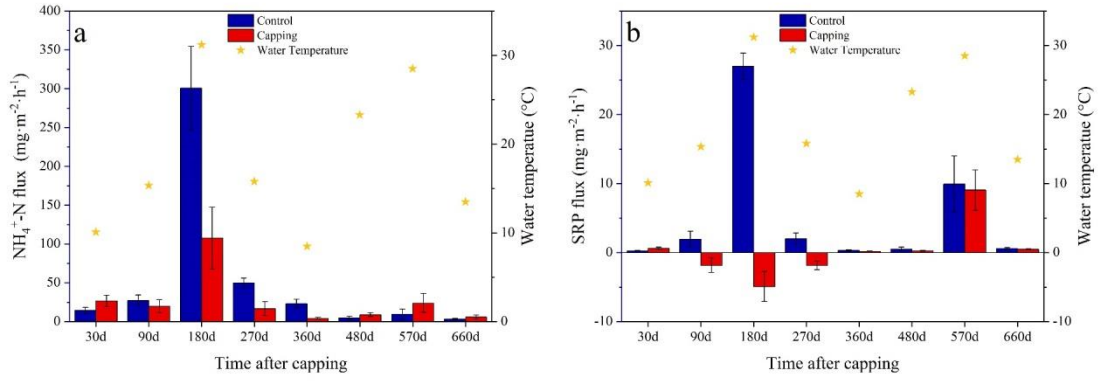
680

Fig. 6. SRP concentration in porewater profiles for control and capping sediment at eleven sampling times.

681

682

683



684

685

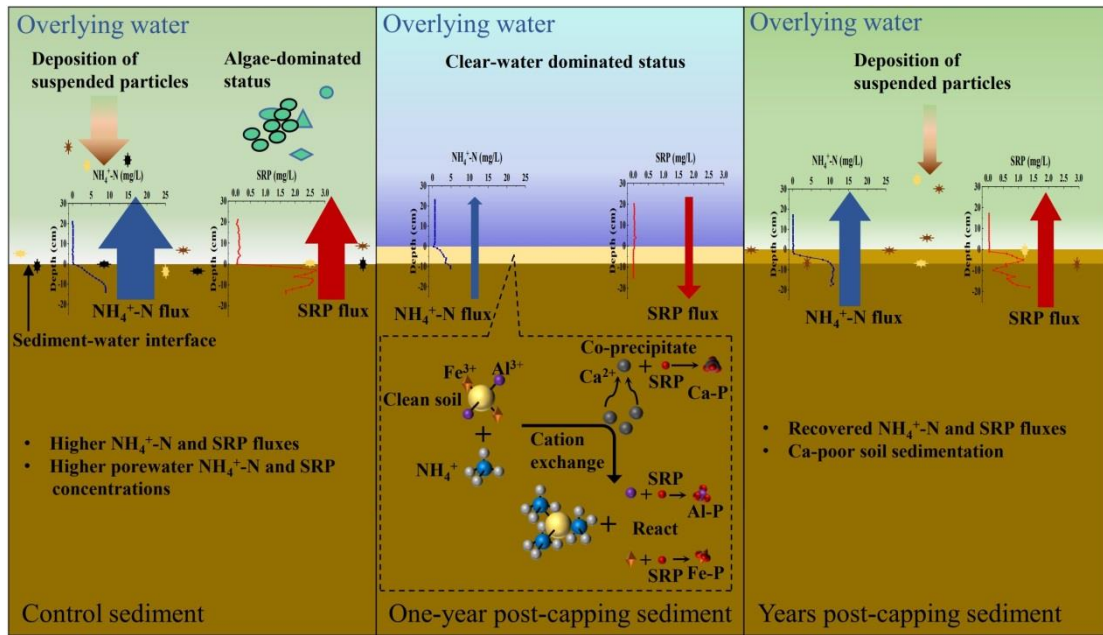
Fig. 7. Diffusive fluxes of $\text{NH}_4^+\text{-N}$ and SRP across the sediment-water interface for control and capping sediment at eight sampling times.

686

687

688

689



690

691 **Fig. 8.** Schematic representation of Ca-poor soil capping in control sediment internal
 692 loading, and the response of overlying water status in temporally.

693

694

695

696 **References**

- 697 Ajmal, Z., Muhmood, A., Usman, M., Kizito, S., Lu, J., Dong, R., Wu, S., 2018.
698 Phosphate removal from aqueous solution using iron oxides: Adsorption,
699 desorption and regeneration characteristics. *J. Colloid Interface Sci.* 528, 145–
700 155.
- 701 Alshameri, A., Ibrahim, A., Assabri, A.M., Lei, X., Wang, H., Yan, C., 2014. The
702 investigation into the ammonium removal performance of Yemeni natural
703 zeolite: Modification, ion exchange mechanism, and thermodynamics. *Powder*
704 *Technol.* 258, 20–31.
- 705 Beutel, M.W., 2006. Inhibition of ammonia release from anoxic profundal sediments
706 in lakes using hypolimnetic oxygenation. *Ecol. Eng.* 28(3), 271–279.
- 707 Blindow, I., 1992. Long- and short-term dynamics of submerged macrophytes in two
708 shallow eutrophic lakes. *Freshwater Biol.* 28(1), 15–27.
- 709 Bullerjahn, G.S., McKay, R.M., Davis, T.W., Baker, D.B., Boyer, G.L., D'Anglada,
710 L.V., Doucette, G.J., Ho, J.C., Irwin, E.G., Kling, C.L., Kudela, R.M.,
711 Kurmayer, R., Michalak, A.M., Ortiz, J.D., Otten, T.G., Paerl, H.W., Qin, B.,
712 Sohngen, B.L., Stumpf, R.P., Visser, P.M., Wilhelm, S.W., 2016. Global
713 solutions to regional problems: Collecting global expertise to address the
714 problem of harmful cyanobacterial blooms. A Lake Erie case study. *Harmful*
715 *Algae* 54, 223–238.
- 716 Cao, D., Jin, X., Gan, L., Wang, T., Chen, Z., 2016. Removal of phosphate using
717 iron oxide nanoparticles synthesized by eucalyptus leaf extract in the presence
718 of CTAB surfactant. *Chemosphere* 159, 23–31.
- 719 Chen, M., Ding, S., Liu, L., Xu, D., Han, C., Zhang, C., 2015. Iron-coupled
720 inactivation of phosphorus in sediments by macrozoobenthos (chironomid
721 larvae) bioturbation: Evidences from high-resolution dynamic measurements.
722 *Environ. Pollut.* 204, 241–247.
- 723 Chinese EPA, 2002. *Methods for the Examination of Water and Wastewater*. China
724 Environmental Science Press: Beijing, China, 243–258.
- 725 Copetti, D., Finsterle, K., Marziali, L., Stefani, F., Tartari, G., Douglas, G., Reitzel,
726 K., Spears, B.M., Winfield, I.J., Crosa, G., D'Haese, P., Yasserli, S., Lüriling,
727 M., 2016. Eutrophication management in surface waters using lanthanum
728 modified bentonite: A review. *Water Res.* 97, 162–174.
- 729 Cotner, J.B., 2017. Nitrogen is Not a 'House of Cards'. *Environ. Sci. Technol.* 51(1),
730 3–3.
- 731 Ding, S., Chen, M., Gong, M., Fan, X., Qin, B., Xu, H., Gao, S., Jin, Z., Tsang,
732 D.C.W., Zhang, C., 2018. Internal phosphorus loading from sediments causes
733 seasonal nitrogen limitation for harmful algal blooms. *Sci. Total Environ.* 625,
734 872–884.
- 735 Figueiredo, C., Grilo, T.F., Oliveira, R., Ferreira, I.J., Gil, F., Lopes, C., Brito, P.,
736 Ré, P., Caetano, M., Diniz, M., Raimundo, J., 2022. Single and combined
737 ecotoxicological effects of ocean warming, acidification and lanthanum
738 exposure on the surf clam (*Spisula solida*). *Chemosphere* 302, 134850.
- 739 Gan, B.K., Madsen, I.C., Hockridge, J.G., 2009. In situ X-ray diffraction of the

740 transformation of gibbsite to α -alumina through calcination: effect of particle
741 size and heating rate. *J. Appl. Crystallogr.* 42(4), 697–705.

742 Gibbs, M.M., Hickey, C.W., 2018. Flocculants and Sediment Capping for
743 Phosphorus management. In *Lake Restoration Handbook*. Springer, Cham, pp.
744 207–265.

745 Gu, B.W., Hong, S.H., Lee, C.G., Park, S.J., 2019. The feasibility of using bentonite,
746 illite, and zeolite as capping materials to stabilize nutrients and interrupt their
747 release from contaminated lake sediments. *Chemosphere* 219, 217–226.

748 Gu, B.W., Lee, C.G., Lee, T.G., Park, S.J., 2017. Evaluation of sediment capping
749 with activated carbon and nonwoven fabric mat to interrupt nutrient release
750 from lake sediments. *Sci. Total Environ.* 599-600, 413–421.

751 Guo, L., 2007. Ecology - Doing battle with the green monster of Taihu Lake.
752 *Science*. 317(5842), 1166–1166.

753 Hinsinger, P., 2001. Bioavailability of soil inorganic P in the rhizosphere as
754 affected by root-induced chemical changes: a review. *Plant soil* 237(2), 173–
755 195.

756 Huser, B.J., Egemose, S., Harper, H., Hupfer, M., Jensen, H., Pilgrim, K.M., Reitzel,
757 K., Rydin, E., Futter, M., 2016. Longevity and effectiveness of aluminum
758 addition to reduce sediment phosphorus release and restore lake water quality.
759 *Water Res.* 97, 122–132.

760 Lai, D.Y.F., Lam, K.C., 2009. Phosphorus sorption by sediments in a subtropical
761 constructed wetland receiving stormwater runoff. *Ecol. Eng.* 35(5), 735–743.

762 Leyva-Ramos, R., Jacobo-Azuara, A., Diaz-Flores, P.E., Guerrero-Coronado, R.M.,
763 Mendoza-Barron, J., Berber-Mendoza, M.S., 2008. Adsorption of chromium
764 (VI) from an aqueous solution on a surfactant-modified zeolite. *Colloids Surf.,*
765 *A* 330(1), 35–41.

766 Li, X., Xie, Q., Chen, S., Xing, M., Guan, T., Wu, D., 2019. Inactivation of
767 phosphorus in the sediment of the Lake Taihu by lanthanum modified zeolite
768 using laboratory studies. *Environ. Pollut.* 247, 9–17.

769 Li, Y., Fan, Y., Li, X., Wu, D., 2017. Evaluation of zeolite/hydrous aluminum oxide
770 as a sediment capping agent to reduce nutrients level in a pond. *Ecol. Eng.* 101,
771 170–178.

772 Lin, J., He, S., Zhang, H., Zhan, Y., Zhang, Z., 2019. Effect of zirconium-modified
773 zeolite addition on phosphorus mobilization in sediments. *Sci. Total Environ.*
774 646, 144–157.

775 Lin, J., Zhan, Y., Zhu, Z., 2011. Evaluation of sediment capping with active barrier
776 systems (ABS) using calcite/zeolite mixtures to simultaneously manage
777 phosphorus and ammonium release. *Sci. Total Environ.* 409(3), 638–646.

778 Lin, L., Lei, Z., Wang, L., Liu, X., Zhang, Y., Wan, C., Lee, D.-J., Tay, J.H., 2013.
779 Adsorption mechanisms of high-levels of ammonium onto natural and
780 NaCl-modified zeolites. *Sep. Purif. Technol.* 103, 15–20.

781 Lin, L., Wan, C., Lee, D.-J., Lei, Z., Liu, X., 2014. Ammonium assists
782 orthophosphate removal from high-strength wastewaters by natural zeolite. *Sep.*
783 *Purif. Technol.* 133, 351–356.

784 Liu, C., Du, Y., Yin, H., Fan, C., Chen, K., Zhong, J., Gu, X., 2019. Exchanges of
785 nitrogen and phosphorus across the sediment-water interface influenced by the
786 external suspended particulate matter and the residual matter after dredging.
787 *Environ. Pollut.* 246, 207–216.

788 Liu, C., Du, Y., Zhong, J., Zhang, L., Huang, W., Han, C., Chen, K., Gu, X., 2022.
789 From macrophyte to algae: Differentiated dominant processes for internal
790 phosphorus release induced by suspended particulate matter deposition. *Water*
791 *Res.* 224, 119067.

792 Liu, C., Zhong, J., Wang, J., Zhang, L., Fan, C., 2016. Fifteen-year study of
793 environmental dredging effect on variation of nitrogen and phosphorus
794 exchange across the sediment-water interface of an urban lake. *Environ. Pollut.*
795 219, 639–648.

796 Lurling, M., Mackay, E., Reitzel, K., Spears, B.M., 2016. Editorial - A critical
797 perspective on geo-engineering for eutrophication management in lakes. *Water*
798 *Res.* 97, 1–10.

799 Moore, B.C., Lafer, J.E., Funk, W.H., 1994. Influence of aquatic macrophytes on
800 phosphorus and sediment porewater chemistry in a freshwater wetland. *Aquat.*
801 *Bot.* 49(2–3), 137–148.

802 Paerl, H.W., Scott, J.T., McCarthy, M.J., Newell, S.E., Gardner, W.S., Havens, K.E.,
803 Hoffman, D.K., Wilhelm, S.W., Wurtsbaugh, W.A., 2016. It Takes Two to
804 Tango: When and Where Dual Nutrient (N & P) Reductions Are Needed to
805 Protect Lakes and Downstream Ecosystems. *Environ. Sci. Technol.* 50(20),
806 10805–10813.

807 Pan, G., Dai, L., Li, L., He, L., Li, H., Bi, L., Gulati, R.D., 2012a. Reducing the
808 Recruitment of Sedimented Algae and Nutrient Release into the Overlying
809 Water Using Modified Soil/Sand Flocculation-Capping in Eutrophic Lakes.
810 *Environ. Sci. Technol.* 46(9), 5077–5084.

811 Pan, G., Dai, L., Li, L., Shang, Y., Li, H., Bi, L., He, L., Wang, L., Wang, D., Li, Q.,
812 Li, L., Gu, X., Zhong, J., Yu, Y., Yan, Q., 2012b. Eutrophication control using
813 modified local soil/sand induced ecological restoration technology: I. Effect
814 and mechanism on short and long term improvement of water quality. *Sci.*
815 *Limnol. Sin.* 24(6), 801–810.

816 Pan, G., Krom, M.D., Zhang, M., Zhang, X., Wang, L., Dai, L., Sheng, Y., Mortimer,
817 R.J.G., 2013. Impact of suspended inorganic particles on phosphorus cycling in
818 the Yellow River (China). *Environ. Sci. Technol.* 47 (17), 9685–9692.

819 Pan, G., Miao, X., Bi, L., Zhang, H., Wang, L., Wang, L., Wang, Z., Chen, J., Ali, J.,
820 Pan, M., Zhang, J., Yue, B., Lyu, T., 2019. Modified Local Soil (MLS)
821 Technology for Harmful Algal Bloom Control, Sediment Remediation, and
822 Ecological Restoration. *Water* 11(6), 1123.

823 Pan, G., Krom, M. D., Herut, B., 2002. Adsorption-Desorption of Phosphate on
824 Airborne Dust and Riverborne Particulates in East Mediterranean Seawater.
825 *Environ. Sci. Technol.* 36(16), 3519–3524.

826 Peterson, S.A., Sanville, W.D., Stay, F.S., Powers, C.F., 1976. Laboratory
827 evaluation of nutrient inactivation compounds for lake restoration. *J. Water*

828 Pollut. Control Fed., 817–831.

829 Qin, B., Xu, P., Wu, Q., Luo, L. Zhang, Y., 2007. Environmental Issues of Lake
830 Taihu, China. In *Eutrophication of shallow lakes with special reference to Lake*
831 *Taihu, China*. Springer, Dordrecht, pp. 3–14.

832 Roberts, K.L., Eate, V.M., Eyre, B.D., Holland, D.P., Cook, P.L.M., 2012. Hypoxic
833 events stimulate nitrogen recycling in a shallow salt-wedge estuary: The Yarra
834 River estuary, Australia. *Limnol. Oceanogr.* 57(5), 1427–1442.

835 Rönicke, H., Frassl, M.A., Rinke, K., Tittel, J., Beyer, M., Kormann, B., Gohr, F.,
836 Schultze, M., 2021. Suppression of bloom-forming colonial cyanobacteria by
837 phosphate precipitation: A 30 years case study in Lake Barleber (Germany).
838 *Ecol. Eng.* 162, 106171.

839 Rukun, L., 1999. *Analytical methods for soil and agricultural chemistry*.
840 *Agricultural Science and Technology Press of China: Beijing*, pp. 15–20.

841 Rydin, E., 2000. Potentially mobile phosphorus in Lake Erken sediment. *Water Res.*
842 34(7), 2037–2042.

843 Sand-Jensen, K., Martinsen, K.T., Jakobsen, A.L., Sjø, J.S., Madsen-Østerbye, M.,
844 Kjær, J.E., Kristensen, E., Kragh, T., 2021. Large pools and fluxes of carbon,
845 calcium and phosphorus in dense charophyte stands in ponds. *Sci. Total*
846 *Environ.* 765, 142792.

847 Scheffer, M., van Nes, E.H., 2007. Shallow lakes theory revisited: various
848 alternative regimes driven by climate, nutrients, depth and lake size.
849 *Hydrobiologia* 584 (1), 455–466.

850 Schnürer, J., Rosswall, T., 1982. Fluorescein diacetate hydrolysis as measure of
851 total microbial activity in soil and litter. *Appl. Environ. Microb.* 43(6), 1256–
852 1256.

853 Shannon, K.E.M., Saleh-Lakha, S., Burton, D.L., Zebarth, B.J., Goyer, C., Trevors,
854 J.T., 2011. Effect of nitrate and glucose addition on denitrification and nitric
855 oxide reductase (cnorB) gene abundance and mRNA levels in *Pseudomonas*
856 *mandelii* inoculated into anoxic soil. *Antonie van Leeuwenhoek.* 100(2), 183–
857 195.

858 Spears, B.M., Maberly, S.C., Pan, G., Mackay, E., Bruere, A., Corker, N., Douglas,
859 G., Egemose, S., Hamilton, D., Hatton-Ellis, T., Huser, B., Li, W., Meis, S.,
860 Moss, B., Lurling, M., Phillips, G., Yasserli, S., Reitzel, K., 2014.
861 Geo-engineering in lakes: a crisis of confidence? *Environ. Sci. Technol.* 48(17),
862 9977–9979.

863 Sun, C., Wang, S., Wang, H., Hu, X., Yang, F., Tang, M., Zhang, M., Zhong, J.,
864 2022. Internal nitrogen and phosphorus loading in a seasonally stratified
865 reservoir: Implications for eutrophication management of deep-water
866 ecosystems. *J. Environ. Manage.* 319, 115681.

867 Sun, S., Huang, S., Sun, X., Wen, W., 2009. Phosphorus fractions and its release in
868 the sediments of Haihe River, China. *J. Environ. Sci.* 21(3), 291–295.

869 Tammeorg, O., Nürnberg, G., Horppila, J., Haldna, M., Niemistö, J., 2020.
870 Redox-related release of phosphorus from sediments in large and shallow Lake
871 Peipsi: Evidence from sediment studies and long-term monitoring data. *J. Great*

872 Lakes Res. 46(6), 1595–1603.

873 Wang, J., Chen, J., Ding, S., Guo, J., Christopher, D., Dai, Z., Yang, H., 2016.

874 Effects of seasonal hypoxia on the release of phosphorus from sediments in

875 deep-water ecosystem: A case study in Hongfeng Reservoir, Southwest China.

876 Environ. Pollut. 219, 858–865.

877 Wang, Y., Ding, S., Wang, D., Sun, Q., Lin, J., Shi, L., Chen, M., Zhang, C., 2017.

878 Static layer: A key to immobilization of phosphorus in sediments amended with

879 lanthanum modified bentonite (Phoslock®). Chem. Eng. J. 325, 49–58.

880 Watson, S.B., Miller, C., Arhonditsis, G., Boyer, G.L., Carmichael, W., Charlton,

881 M.N., Confesor, R., Depew, D.C., Höök, T.O., Ludsin, S.A., Matisoff, G.,

882 McElmurry, S.P., Murray, M.W., Peter Richards, R., Rao, Y.R., Steffen, M.M.,

883 Wilhelm, S.W., 2016. The re-eutrophication of Lake Erie: Harmful algal

884 blooms and hypoxia. Harmful Algae 56, 44–66.

885 Wen, S., Zhong, J., Li, X., Liu, C., Yin, H., Li, D., Ding, S., Fan, C., 2020. Does

886 external phosphorus loading diminish the effect of sediment dredging on

887 internal phosphorus loading? An in-situ simulation study. J. Hazard. Mater. 394,

888 122548.

889 Wu, Z., Wang, C., Jiang, H., Li, K., Yang, X., Huang, W., 2022. Sediment pH

890 structures the potential of the lake's internal P pollution involved in different

891 types of P reactivation. J. Cleaner Prod. 352, 131576.

892 Xu, R., Zhang, M., Mortimer, R.J.G., Pan, G., 2017. Enhanced Phosphorus Locking

893 by Novel Lanthanum/Aluminum–Hydroxide Composite: Implications for

894 Eutrophication Control. Environ. Sci. Technol. 51(6), 3418–3425.

895 Yang, C., Yang, P., Geng, J., Yin, H., Chen, K., 2020. Sediment internal nutrient

896 loading in the most polluted area of a shallow eutrophic lake (Lake Chaohu,

897 China) and its contribution to lake eutrophication. Environ. Pollut. 262,

898 114292.

899 Yin, H., Yang, C., Yang, P., Kaksonen, A.H., Douglas, G.B., 2021. Contrasting

900 effects and mode of dredging and in situ adsorbent amendment for the control

901 of sediment internal phosphorus loading in eutrophic lakes. Water Res. 189,

902 116644.

903 Yu, J., Ding, S., Zhong, J., Fan, C., Chen, Q., Yin, H., Zhang, L., Zhang, Y., 2017.

904 Evaluation of simulated dredging to control internal phosphorus release from

905 sediments: Focused on phosphorus transfer and resupply across the

906 sediment-water interface. Sci. Total Environ. 592, 662–673.

907 Zhan, Y., Yu, Y., Lin, J., Wu, X., Wang, Y., Zhao, Y., 2019. Simultaneous control

908 of nitrogen and phosphorus release from sediments using iron-modified zeolite

909 as capping and amendment materials. J. Environ. Manage. 249, 109369.

910 Zhang, H., Lyu, T., Liu, L., Hu, Z., Chen, J., Su, B., Yu, J., Pan, G., 2021. Exploring

911 a multifunctional geoengineering material for eutrophication remediation:

912 Simultaneously control internal nutrient load and tackle hypoxia. Chem. Eng. J.

913 406, 127206.

914 Zhong, J.C., Yu, J.H., Zheng, X.L., Wen, S.L., Liu, D.H., Fan, C.X., 2018. Effects

915 of Dredging Season on Sediment Properties and Nutrient Fluxes across the

916 Sediment–Water Interface in Meiliang Bay of Lake Taihu, China. *Water* 10(11),
917 1606.

918 Zhong, J., Chen, C., Yu, J., Shen, Q., Liu, C., Fan, C., 2022. Effect of dredging and
919 capping with clean soil on the mitigation of algae-induced black blooms in
920 Lake Taihu, China: A simulation study. *J. Environ. Manage.* 302, 114106.

921 Zhong, J., Fan, C., Liu, G., Zhang, L., Shang, J., Gu, X., 2010a. Seasonal variation
922 of potential denitrification rates of surface sediment from Meiliang Bay, Taihu
923 Lake, China. *J. Environ. Sci.* 22(7), 961–967.

924 Zhong, J., Fan, C., Zhang, L., Hall, E., Ding, S., Li, B., Liu, G., 2010b. Significance
925 of dredging on sediment denitrification in Meiliang Bay, China: A year-long
926 simulation study. *J. Environ. Sci.* 22(1), 68–75.

927 Zhong, J., Wen, S., Zhang, L., Wang, J., Liu, C., Yu, J., Zhang, L., Fan, C., 2021.
928 Nitrogen budget at sediment–water interface altered by sediment dredging and
929 settling particles: Benefits and drawbacks in managing eutrophication. *J.*
930 *Hazard. Mater.* 406, 124691.

931 Zhou, J., Li, D., Chen, S., Xu, Y., Geng, X., Guo, C., Huang, Y., 2019. Sedimentary
932 phosphorus immobilization with the addition of amended calcium peroxide
933 material. *Chem. Eng. J.* 357, 288–297.

934

935